

Mid- and Far-IR Spectra of H_5^+ and D_5^+ Compared to the Predictions of Anharmonic Theory

Timothy C. Cheng,[†] Ling Jiang,[‡] Knut R. Asmis,[‡] Yimin Wang,[§] Joel M. Bowman,[§] Allen M. Ricks,[†] and Michael A. Duncan^{*,†}

[†]Department of Chemistry, University of Georgia, Athens, Georgia 30602, United States

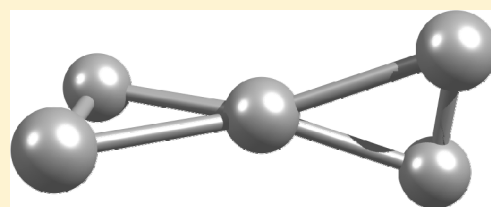
[‡]Fritz-Haber-Institut der Max-Planck-Gesellschaft, Faradayweg 4-6, 14195 Berlin, Germany

[§]Department of Chemistry, Emory University, Atlanta, Georgia 30332, United States

S Supporting Information

ABSTRACT: H_5^+ is the smallest proton-bound dimer. As such, its potential energy surface and spectroscopy are highly complex, with extreme anharmonicity and vibrational state mixing; this system provides an important benchmark for modern theoretical methods. Unfortunately, previous measurements covered only the higher-frequency region of the infrared spectrum. Here, spectra for H_5^+ and D_5^+ are extended to the mid- and far-IR, where the fundamental of the proton stretch and its combinations with other low-frequency vibrations are expected. Ions in a supersonic molecular beam are mass-selected and studied with multiple-photon dissociation spectroscopy using the FELIX free electron laser. A transition at 379 cm^{-1} is assigned tentatively to the fundamental of the proton stretch of H_5^+ , and bands throughout the $300\text{--}2200\text{ cm}^{-1}$ region are assigned to combinations of this mode with bending and torsional vibrations. Coupled vibrational calculations, using ab initio potential and dipole moment surfaces, account for the highly anharmonic nature of these complexes.

SECTION: Spectroscopy, Photochemistry, and Excited States



Small hydrogen ions and their clusters have been seen for many years in plasma and mass spectrometry environments.^{1–3} These fascinating ions are also believed to be present in interstellar gas clouds, playing a vital role in the chemistry at low temperature.^{4–7} H_3^+ was first observed over 100 years ago by J. J. Thomson in hydrogen discharges.⁸ Since then, this ion has been studied extensively because of the low proton affinity of H_2 and the consequent tendency of H_3^+ to undergo proton-transfer reactions.^{9–18} Larger protonated hydrogen clusters such as H_5^+ were also observed, and their chemistry has also been documented.^{19–21} The laboratory infrared spectrum of H_3^+ was reported by Oka and co-workers,^{22,23} and subsequently this ion was identified in numerous interstellar sources.^{24–27} H_5^+ is the intermediate in the symmetric proton transfer from H_3^+ to H_2 , and its deuterated analogues are proposed as intermediates in deuterium fractionation reactions in the interstellar medium.^{15–17,26,27} After much computational study, H_5^+ , in its ground vibrational state, is recognized as a symmetric (D_{2d}) proton-bound dimer.^{28–44} Its potential has a double minimum with limiting $H_3^+H_2$ structures, but the maximum of the zero-point density is located at the D_{2d} first-order saddle point, giving rise to a symmetric structure with an equally shared proton. Okumura, Yeh, and Lee (OYL) reported the first IR spectroscopy for H_5^+ in the $3500\text{--}4000\text{ cm}^{-1}$ region,^{45,46} but assignment of the bands was complicated by the extreme anharmonicity of the system. More recently, Cheng et al. used more efficient ion cooling and broader IR laser tuning ($2000\text{--}4500\text{ cm}^{-1}$) to obtain improved data for H_5^+ and the

first spectra for D_5^+ .⁴⁷ These spectra were assigned in coordination with a full anharmonic potential and spectral analysis. In the present Letter, these latter measurements are extended for both H_5^+ and D_5^+ into the mid- and far-IR region using the expanded frequency coverage of the FELIX free electron laser.⁴⁸

The infrared spectrum of H_5^+ measured by OYL used mass selection of the ion followed by laser photodissociation measurements, detecting the yield of H_3^+ ions resulting from the elimination of H_2 .^{45,46} Three broad asymmetric bands in the $3450\text{--}4150\text{ cm}^{-1}$ region were assigned to vibrations involving shared-proton and terminal H_2 stretching motions. Our latest measurements used the expanded tuning range of new IR-OPO lasers to cover the $2000\text{--}4500\text{ cm}^{-1}$ region.⁴⁷ We detected the bands seen originally by OYL, as well as an additional feature at 2603 cm^{-1} . Our spectra were the first for D_5^+ , producing several bands in the $2500\text{--}3200\text{ cm}^{-1}$ region.⁴⁷ Using Diffusion Monte Carlo (DMC) and vibrational configuration interaction [the “Reaction Path” version of the code MULTIMODE (MM-RPH)] calculations, the spectra for both H_5^+ and D_5^+ were assigned and found to be in good agreement with the predicted spectrum, corresponding to the D_{2d} symmetry structure.⁴⁷

Received: August 27, 2012

Accepted: October 15, 2012

Published: October 15, 2012



The previous spectroscopy of H_5^+ focused on the high-frequency region of the infrared. Because the density of mass-selected ions is too low for absorption spectroscopy, photodissociation measurements were employed, which are most effective at energies above the one-photon dissociation threshold. Experimental dissociation energies of H_5^+ (to eliminate H_2) have been measured between 5.0 and 10.0 kcal/mol, (1750–3500 cm^{-1}), with the most recent value at 6.9 kcal/mol (2415 cm^{-1}).¹⁹ DMC calculations find $D_0 = 6.37$ and 6.87 kcal/mol for H_5^+ and D_5^+ ions, respectively (2227 and 2402 cm^{-1}).^{36,47} Our single-photon photodissociation experiments found bands beginning just above these two predicted thresholds, but none below, consistent with the DMC results. To provide a more complete picture of the vibrational dynamics in this prototype system, measurements are needed at longer wavelengths. In the mid- and far-IR regions, the fundamental of the proton stretch vibration and other low-lying overtone and combination bands are predicted. Unfortunately, spectroscopy at such low energies is extremely challenging because of the limited coverage of available IR lasers and the difficulty of detection schemes. Measurement of IR photodissociation spectra below the bond-breaking threshold requires either tagging with a so-called “messenger atom” (typically neon or argon)^{49–53} or resonance-enhanced multiple-photon dissociation (IR-MPD).^{54–56} Tagging in a delicate system like H_5^+ is undesirable as the tag atom binding energy and mass relative to the system would likely introduce significant perturbations on the native vibrational structure. Multiple-photon dissociation generally requires higher laser fluences than those available from OPO sources, particularly in the region below 2000 cm^{-1} . Therefore, we have employed the FELIX free electron laser,⁴⁸ located at the F.O.M. Laboratory for Plasma Physics in Nieuwegein, The Netherlands, for these experiments. This laser provides the tuning range in the mid- and far-IR with the fluence required for IR-MPD measurements.

The mass spectrum of the ions produced in this experiment contains primarily protonated hydrogen clusters of the form $\text{H}_{(2n+1)}^+$ ($n \geq 1$). As noted before,⁴⁷ the intensities of these peaks drop drastically after H_9^+ . This is not surprising because previously computed structures show that three hydrogen molecules bind to a H_3^+ core ion, with one on each corner forming the first solvation shell.^{30–34} Binding energies for subsequent hydrogen molecules drop substantially after this $\text{H}_3^+(\text{H}_2)_3$ shell closing,¹⁹ consistent with the computed structures and with the mass spectrum.

Figure 1 shows the infrared photodissociation yield of mass-selected H_5^+ from 300 to 2100 cm^{-1} measured in the H_3^+ mass channel corresponding to the loss of H_2 (top trace). Remarkably, multiple-photon fragmentation occurs throughout this region. At frequencies above 1114 cm^{-1} , dissociation is a two-photon process (derived from the computed dissociation energy), while in the region of 742–1114 cm^{-1} , it is a three-photon process, and so on for lower frequencies. The signal is significantly weaker in the lower-frequency region, indicating that only two- and three-photon processes occur with reasonable efficiency. The dissociation yield has a broad underlying background, whose intensity is a few percent of that of resonant features, probably due to a fraction of ions not cooled completely. Superimposed on this are several peaks with higher yields, consistent with resonance-enhanced MPD. The most intense bands occur at 940 and 1399 cm^{-1} , whereas much weaker features appear at 320, 379, 470, 1180, 1723, and 1952

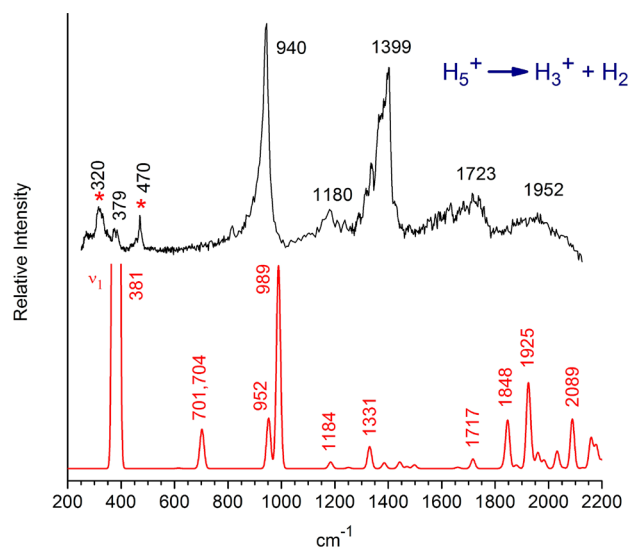


Figure 1. Experimental IR-MPD spectrum of $\text{H}_5^+ \rightarrow \text{H}_3^+ + \text{H}_2$ in the range of 300–2200 cm^{-1} (top trace) versus the predicted theoretical spectrum (bottom, red). The theoretical spectrum has intensities determined by the one-photon IR absorption strength, while the measured spectrum comes from multiple photon absorption, whose order varies across the spectrum.

cm^{-1} . According to the well-known mechanism of IR-MPD, vibrational fundamentals are excited initially followed by continued absorption to higher vibrational levels if enough state density is available to support the process.^{54–56} The occurrence of peaks is therefore associated with vibrational absorption bands, but their positions and intensities may be shifted somewhat relative to those expected for one-photon absorption.⁵⁷ Note, the band contours with a pronounced tail to lower energies seen here are not necessarily due to the MPD mechanism as similar widths and profiles were observed in the previous single-photon measurements for H_5^+ and attributed to the rotational contours of these bands.^{45–47} The 940 cm^{-1} resonance is necessarily the result of a three-photon process, while the 1399 cm^{-1} feature can be produced via a two-photon process. Therefore, the actual absorption probability for the 940 cm^{-1} band is likely much greater than that of the 1399 cm^{-1} band, consistent with computed intensities (see below). The weak bands at 320 and 470 cm^{-1} likely arise from an artifact attributed to leakage of higher harmonics of the FELIX fundamental.⁵⁸ These bands occur at nearly 1/3 of the frequency of the strong 940 and 1399 cm^{-1} bands and are therefore attributed to similar transitions excited by the third harmonic of FELIX. The 379 cm^{-1} band lacks any corresponding band at three times its energy and is believed to be a “real” feature, although it is extremely weak.

As described in our previous paper,⁴⁷ the DMC/reaction path/MULTIMODE (MM-RPH) methodology finds a symmetric D_{2d} structure for the H_5^+ and D_5^+ ions. The present work is based primarily on MM-RPH calculations. In this approach, a torsional mode, describing the mutual twist of the two outer H_2 groups is coupled to normal modes orthogonal to the torsional path. One of the modes describes the proton transfer between the two H_2 groups. For technical reasons, the reference geometry for this calculation is the second-order saddle point of D_{2h} symmetry and not the first-order saddle point of D_{2d} symmetry. Thus, the relevant eight vibrational modes for analysis of molecular eigenstates are those of the

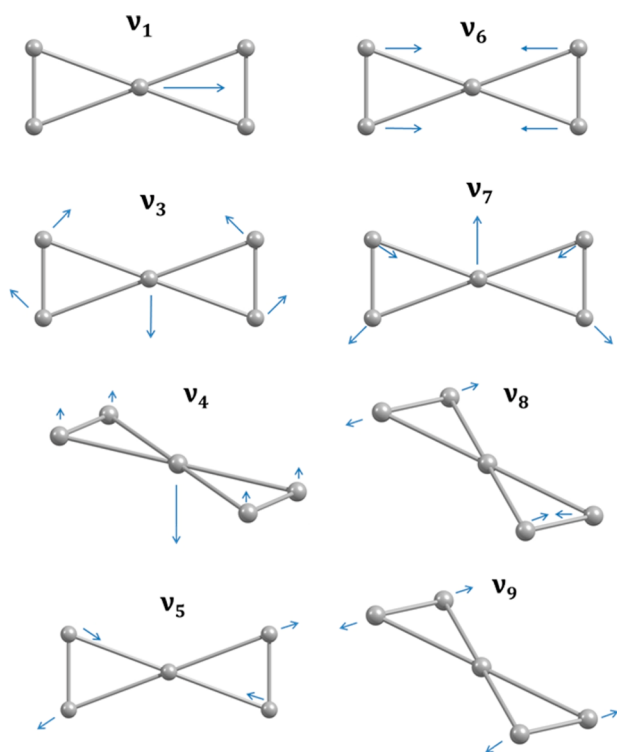


Figure 2. Selected vibrational modes of H_5^+ relevant for this study.

second-order saddle point; these are shown in Figure 2. Note that the “missing” ninth mode is the torsion, and the shared proton-transfer mode, ν_1 , is an imaginary-frequency mode. The modes at this reference configuration do transform according to the irreducible representations of the D_{2d} point group; however, the calculations use reduced D_2 symmetry. In that symmetry, the modes shown in Figure 2 transform as follows: [τ, ν_5, ν_8]- a_1 ; [ν_1, ν_7]- b_3 ; [ν_2, ν_6]- b_2 ; [ν_3, ν_4]- b_1 . The PES and dynamics do indicate that the relevant point group is D_{2db} as already noted, and thus the irreducible representations for that group are the appropriate ones. In particular, there should be two sets of e modes for D_{2db} as reported by Yamaguchi et al.²⁸ We do observe this degeneracy approximately, and we point this out below.

As is typical for proton-bound dimers,⁵⁷ the shared proton-transfer mode has a large dipole intensity and is markedly anharmonic, and therefore states that are mixed with this mode also show significant IR intensity. The most intense vibrational lines of H_5^+ are shown in Table 1, together with their expansion coefficients in terms of a zero-order basis that includes the torsional mode. To be perfectly clear, these are the coefficients in the standard expansion of the molecular eigenstate in terms of the zero-order basis. (The squares of these coefficients correspond to the fraction of the zero-order states that contribute to the molecular eigenstates.) Note, in most cases the coefficients are quite small, indicating significant mixing using this zero-order basis, which consists of 30 000 terms. A more complete listing of energies and assignments of the 50 lowest-lying bands is given in the Supporting Information (SI) for this Letter. As seen, many of the states show significant mixing with ν_1 , the proton-transfer mode, which is predicted to occur at 381 cm^{-1} . This mode was found at 334 cm^{-1} in the previous fixed node DMC calculations.⁴⁷ As seen, the MM-RPH result for this important mode is roughly 45 cm^{-1} higher than the DMC value. The energy of this fundamental has been

Table 1. Predicted Vibrational Bands for H_5^+ , Their Intensities, and the Mixed Vibrational Character Giving Rise to Each

band (cm^{-1})	intensity (km/mol)	leading coefficients	vibrational character
381	1866.9	-0.7442 -0.3165	ν_1 $\nu_1 + \nu_6$
701	7.78	0.6761 0.1773	ν_3 $2\nu_1 + \nu_3$
704	11.99	0.6608 0.2148	ν_4 $2\nu_1 + \nu_4$
952	24.14	-0.7666 -0.2879	$\nu_1 + 4\tau$ $\nu_1 + \nu_6 + 4\tau$
989	99.63	0.3871 -0.3371	ν_1 $\nu_1 + 4\tau$
1184	3.08	0.5618 0.4243	ν_4 ν_5
1331	9.56	0.3820 -0.3587	ν_1 $\nu_3 + \nu_4 + \tau$
1717	0.00	-0.5016 0.3756	$2\nu_1$ $2\nu_4$
1848	23.0	-0.5315 -0.2546	$\nu_1 + 2\nu_3$ $\nu_1 + 2\nu_4$
1925	40.5	-0.6417 -0.2427	$\nu_3 + \nu_4 + \tau$ $\nu_4 + \nu_7$
2032	9.1	0.3851 0.3180	$\nu_3 + 6\tau$ $\nu_7 + 3\tau$
2089	24.3	-0.3347 0.2749	$\nu_3 + \nu_4 + 3\tau$ $\nu_1 + 2\nu_4 + 2\tau$
2159	14.9	-0.5859 -0.2421	$\nu_1 + \nu_6$ $\nu_3 + \nu_4 + \tau$
2178	9.9	-0.3588 0.3382	$\nu_3 + \nu_4 + 3\tau$ $\nu_1 + 2\nu_3 + 4\tau$

calculated recently using MCTDH calculations on the same potential⁴⁴ and reported to be 359 cm^{-1} . (It should be noted that those calculations were for H_5^+ only and did not extend above 1029 cm^{-1} , and intensities were not reported. Thus, it is not possible to comment meaningfully on the relevance of those calculations to the present study, which focus on the prominent features in the experimental spectrum. A detailed comparison of the two sets of calculations is beyond the scope of this Letter.) Based on this and the DMC result, we conclude that the present MM-RPH energy for ν_1 is likely high (for the given PES) by 20–45 cm^{-1} . States with a significant component of one quanta in this mode are probably also high by a similar amount. With this in mind, consider the one-photon absorption spectrum shown in the bottom trace of Figure 1. It is convoluted using a Gaussian line shape function with a width of 7.5 cm^{-1} (fwhm) to facilitate the comparison with experiment.

As indicated, the most intense absorption band is predicted for the ν_1 proton stretch fundamental at 381 cm^{-1} . This band is far off scale in the figure because of its high oscillator strength (1866.9 km/mol). Because the 320 and 470 cm^{-1} bands are artifacts, the only real signal in this region is the band at 379 cm^{-1} , and therefore we tentatively assign this as the ν_1 proton stretch fundamental. The computed intensity of this band is much greater than that of the asymmetric stretch of H_3^+ (206.8 km/mol at the MP2/6-311G+(d,p) level), which has been used for interstellar detection of this ion.^{24–27} Other relatively intense vibrations are predicted and observed in the 900 and

1400 cm^{-1} regions. All these vibrations have highly mixed character, with significant contributions from the proton stretch and its combinations with other modes. Their assignments are indicated in Table 1. Other than the ν_1 proton stretch, the torsional vibration (τ) occurs most often in these combinations. The overtone of the proton stretch ($2\nu_1$) is IR-forbidden by symmetry but is predicted to occur at 1717 cm^{-1} , illustrating the strong negative anharmonicity of the proton stretch potential. The second overtone ($3\nu_1$) was observed at 2603 cm^{-1} in our previous single-photon photodissociation study of the high-frequency spectrum.⁴⁷ As shown in Figure 1, all the experimental features correspond to bands predicted by theory to have significant IR intensity. Conversely, for every strong band predicted, the experiment measures significant dissociation signal nearby. The 940 cm^{-1} band, which has ν_1 mixed with four quanta of the torsion, has lower actual relative intensity than that predicted because it requires a three-photon absorption event. (It might be expected that a state with one quanta of proton stretch and two quanta of torsion would also be intense; however, we do not find this. The reason is that the molecular eigenstates are not well-described by the zero-order basis. The state labeled $\nu_1 + 4\tau$ also has a significant contribution from the intense zero-order ν_1 state, whereas the state $\nu_1 + 2\tau$ does not.) This likely prevents detection of the weaker ν_3/ν_4 bands predicted near 701/704 cm^{-1} . The bands near 1900 cm^{-1} are measured lower than their predicted relative intensity, perhaps because the IR laser output is diminished in this region (we do not normalize to the laser power because of the multiphoton process involved; the laser power variation is shown in Figure S1 in the SI). Overall, the predicted versus experimental spectra are in reasonable agreement, considering the dynamics of the photodissociation process at work here. This seems to indicate that the vibrational band predictions based on MM-RPH calculations are reliable. Note the near degeneracy of the energies of ν_3 and ν_4 in Table 1 (and also in Table 2). This is an example of the relevance of the D_{2d} symmetry, which is only numerically taken into account in our calculations, as noted above.

The IR-MPD spectrum of D_5^+ is shown in the top trace of Figure 3, measuring the intensity of the D_3^+ photofragment ion as a function of wavelength. Again, the theoretical spectrum is shown in the bottom trace, and the character of the vibrations is indicated in Table 2. The difference between the MM-RPH and DMC fundamental of the D^+ -transfer mode is roughly 35 cm^{-1} , and therefore spectral features with significant contribution from this mode are expected to be high by roughly this amount. States involving the overtone of this mode are probably calculated too high by roughly 1–2 times the difference for the fundamental. As seen for H_5^+ , the theoretical spectrum features many combinations with the deuteron stretch, and again the torsional vibration occurs frequently. The fundamental of the ν_1 deuteron stretch for D_5^+ is predicted near 256 cm^{-1} (the DMC value for this fundamental is 222 cm^{-1}). This wavelength is at the lower limit of the FEL range, and no fragmentation is observed here. Indeed, no significant fragmentation signal is detected until the 1200–1800 cm^{-1} region. The prominent band at 1767 cm^{-1} has a position roughly a factor of $2^{-1/2}$ below the $3\nu_1$ band seen for H_5^+ at 2603 cm^{-1} ,⁴⁷ and it is therefore tempting to associate this with the corresponding vibration in D_5^+ . Theory shows that there is indeed a strong component of $3\nu_1$ for the bands in this region, although their character is mixed with that of other vibrations. Except for the signal near 1800 cm^{-1} , there is poorer agreement here between

Table 2. Predicted Vibrational Bands for D_5^+ , Their Intensities, And the Mixed Vibrational Character Giving Rise to Each

band (cm^{-1})	intensity (km/mol)	leading coefficients	vibrational character
256	935.2	−0.8128 −0.3159	ν_1 $\nu_1 + \nu_6$
591	3.89	0.8461 −0.2688	ν_4 $\nu_4 + 2\tau$
595	3.73	0.8561 0.2396	ν_3 $\nu_3 + 2\tau$
827	55.57	0.4959 −0.3903	ν_1 $\nu_1 + \nu_6$
974	8.91	−0.5350 0.4675	$\nu_7 + \tau$ $\nu_3 + 4\tau$
990	6.97	0.5881 0.3640	$\nu_5 + 2\tau$ $\nu_1 + \nu_3 + 3\tau$
1196	8.10	0.7417 0.2257	$\nu_3 + \nu_4 + \tau$ $2\nu_1 + \nu_3 + \nu_4 + \tau$
1241	0.00	−0.5095 0.3450	$2\nu_1$ $2\nu_3 + \tau$
1533	17.01	0.4105 −0.3975	$\nu_1 + \nu_6$ $\nu_4 + \nu_7$
1536	6.64	−0.6065 0.2254	$\nu_1 + 2\nu_4 + 2\tau$ $\nu_1 + 2\nu_4 + 4\tau$
1731	17.01	−0.3390 −0.3330	$3\nu_1$ $\nu_3 + \nu_5 + 3\tau$
1821	17.66	0.3272 −0.3556	$\nu_1 + 2\nu_3 + 4\tau$ $3\nu_1$
1834	27.54	−0.3364 −0.3339	$\nu_1 + 2\nu_3 + 4\tau$ $\nu_1 + 2\nu_4 + 4\tau$
		0.3653 0.3333	$3\nu_1$ $\nu_3 + \nu_4 + 5\tau$

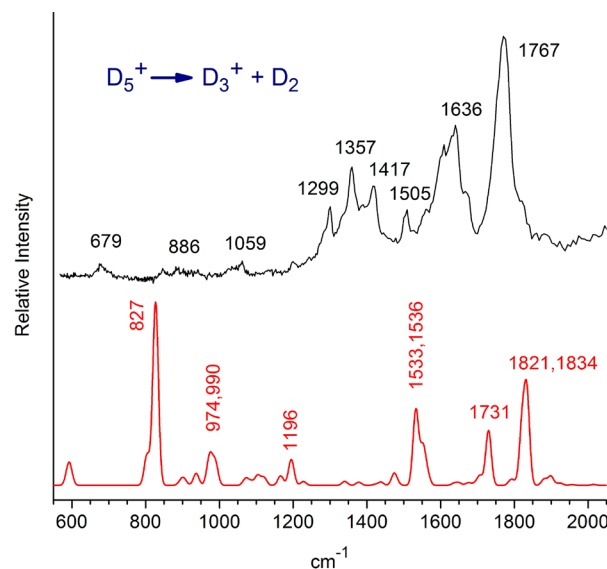


Figure 3. Experimental IR-MPD spectrum of $D_5^+ \rightarrow D_3^+ + D_2$ in the range of 550–2100 cm^{-1} (top trace) versus the predicted spectrum (bottom, red). The theoretical spectrum has intensities determined by the one-photon IR absorption strength, while the measured spectrum comes from multiple photon absorption, whose order varies across the spectrum.

theory and experiment than in the case of H_5^+ . A strong vibration is predicted at 827 cm^{-1} but not detected. Although a

resonance here would require at least four-photon absorption for dissociation, some signal might be expected on the basis of the behavior of H_5^+ above. However, the predicted intensity is about half that of the 940 cm^{-1} band. Likewise, bands predicted near 1196 and 1534 cm^{-1} do not correspond with any measured signals. The second-most intense experimental band at 1636 cm^{-1} could correspond to either the $1533/1536$ or 1731 cm^{-1} predictions, but it is impossible to tell which, if either, is the correct match. Signals at 1299 , 1357 , and 1417 cm^{-1} do not match any predictions. Although this seems unlikely, these signals could be due in part to coherent multiphoton transitions to resonances observed previously with one-photon excitation in the $2500\text{--}3100\text{ cm}^{-1}$ range.⁴⁷ The weaker band predicted at 1196 cm^{-1} lies just below the two-photon threshold, perhaps explaining how it could be missed, but all the other missing bands here are above this threshold.

Comparing these spectra directly, therefore, it seems that the agreement between theory and experiment is worse for the D_5^+ spectrum than it is for that of H_5^+ . However, the disparity may not be quite as bad as it first seems. In the higher-frequency region of the D_5^+ spectrum, where two-photon processes are possible and stronger signal is detected, all the bands predicted have strong contributions from the deuteron stretch, including multiple quanta of this for the 1731 and $1821/1834\text{ cm}^{-1}$ bands. As noted already, this mode is overestimated by our methods, and the errors multiply with the number of quanta in this mode. Inspection of Figure 3 shows that a small down-shift of the predicted bands in this region would bring these more into alignment with the three main experimental band groups.

Other considerations may also affect the spectra for H_5^+ and D_5^+ differently. For example, the specific vibrational dynamics of these two ions may affect their detection efficiency. Because of individual resonances and couplings in these systems, the character of the strong vibrations is not the same, and these fall at different positions relative to the respective two- and three-photon dissociation thresholds. H_5^+ has stronger bands predicted near the two-photon threshold, which are detected. D_5^+ has weaker bands at lower frequencies, which are not detected, probably because of the higher dissociation energy. The stronger D_5^+ bands above the two-photon threshold have multiple-quanta proton stretch character, which are therefore shifted more from the values predicted by theory. Other differences may arise from the IR-MPD method. It is actually quite remarkable that IR-MPD can be detected for this system; the light atoms produce a sparse vibrational state density which is a severe disadvantage for multiple photon processes. In such systems, IR-MPD may cause significant spectral broadening and line shifting relative to one-photon absorption spectra because of its sensitivity to vibrational state density at levels beyond the fundamental. For example, in the related system of the proton-bound water dimer, the IR-MPD spectra had complex patterns⁵⁹ which became simpler when the system was studied with single-photon methods.⁶⁰ The single-photon spectra eventually were in good agreement with the predictions of full-dimensional anharmonic theory.⁶¹ The state density is greater for D_5^+ than for H_5^+ because of its lower-frequency vibrations, which should improve the efficiency of MPD, but the density in both cases is probably low enough that accidental resonances may affect the spectra. Finally we note that there is a proton/hydrogen exchange saddle point at around 1550 cm^{-1} above the global minimum. The current MM-RPH calculations cannot describe this exchange and this could be a source of some error at the highest energies of interest here. (We did

examine this process for the zero-point state in the DMC calculations and found that it was very rare.)

Although questions remain about the spectroscopy of this system, several interesting insights are already clear. The spectrum of H_5^+ is dominated by the proton stretch vibration, which occurs as a strong fundamental and induces activity in combination bands throughout the mid-IR. The torsional vibration features prominently in these combinations, as do several hydrogen bending modes. The proton stretch fundamental has extremely high IR intensity, suggesting that this band in the far-IR should be the target for interstellar searches for this ion. In the mid-IR, theory and experiment agree on the position of other bands with reasonable intensities at 940 cm^{-1} for H_5^+ and 1767 cm^{-1} band for D_5^+ ; these features can provide a guide for higher-resolution experiments in the future. H_5^+ and D_5^+ have surprisingly rich spectra in the mid- and far-IR, representing challenging problems for anharmonic theory and spectroscopy worth continued attention.

METHODS

Cluster ions for this experiment are produced with an electron beam source with excitation of the output of a pulsed valve (Amsterdam cantilever piezo design).⁶² The expansion gas of pure hydrogen included water at its ambient vapor pressure seeded in helium. Experiments employed a ring electrode trap/time-of-flight mass spectrometer described previously.^{63,64} Mass-selected ions are excited with the tunable output of FELIX.⁴⁸ The output of FELIX provides tunable IR light ranging from 300 to 2100 cm^{-1} with pulse energies ranging from 12 to 60 mJ/pulse , depending on the wavelength. Because of the nature of the light source, the line width varies depending on the wavelength, averaging approximately $0.3\text{--}0.5\%$ RMS of the central wavelength. The normalized fragment ion yield is determined from the intensities of the parent and fragment ions and plotted versus the IR photon energy to obtain an IR-MPD spectrum.

The anharmonic, coupled vibrational calculations, ab initio potential energy and dipole moment surfaces were described in detail previously, and therefore we refer the reader to refs 36, 39, and 47 for details. In particular, the details of the MM-RPH calculations were given in the Supporting Information of ref 47. Also, we include energies and assignments of the 50 lowest-lying energies in Table S1 of the SI of this Letter.

ASSOCIATED CONTENT

Supporting Information

First 50 eigenstates of the MM-RPH calculation for H_5^+ and spectra measured for H_5^+ and D_5^+ . This material is available free of charge via the Internet at <http://pubs.acs.org>.

AUTHOR INFORMATION

Corresponding Author

*E-mail: maduncan@uga.edu.

Notes

The authors declare no competing financial interest.

ACKNOWLEDGMENTS

We gratefully acknowledge support for this work by the National Science Foundation through Grant Nos. CHE-0956025 (M.A.D.) and CHE-1145227 (J.M.B.). We would also like to thank the Stichting voor Fundamenteel Onderzoek der Materie (FOM) for beam time at FELIX and the FELIX

staff for support and assistance. This research is funded by the European Community's Seventh Framework Programme (FP7/2007-2013) Grant No. 226716. L.J. thanks the Alexander von Humboldt Foundation for a postdoctoral scholarship.

REFERENCES

- (1) Dawson, P. H.; Tickner, A. W. Detection of H_5^+ in Hydrogen Glow Discharge. *J. Chem. Phys.* **1962**, *37*, 672–673.
- (2) Buchheit, K.; Henkes, W. Mass Spectra of Energy-Analyzed Hydrogen Cluster Ions. *Z. Angew. Phys.* **1968**, *24*, 191–196.
- (3) Clampitt, R.; Gowland, L. Clustering of Cold Hydrogen Gas on Protons. *Nature* **1969**, *223*, 815–816.
- (4) Herbst, E.; Klemperer, W. Formation and Depletion of Molecules in Dense Interstellar Clouds. *Astrophys. J.* **1973**, *185*, 505–533.
- (5) Duley, W. W. Molecular Clusters in Interstellar Clouds. *Astrophys. J. Lett.* **1996**, *471*, L57–L60.
- (6) Roberts, H.; Herbst, E.; Millar, T. J. Enhanced Deuterium Fractionation in Dense Interstellar Cores Resulting from Multiply Deuterated H_3 . *Astrophys. J.* **2003**, *591*, L41–44.
- (7) Roberts, H.; Herbst, E.; Millar, T. J. The Chemistry of Multiply Deuterated Species in Cold, Dense Interstellar Cores. *Astron. Astrophys.* **2004**, *424*, 905–918.
- (8) Thomson, J. J. XXVI. Rays of Positive Electricity. *Philos. Mag.* **1911**, *21*, 225–249.
- (9) Bennett, S. L.; Field, F. H. Reversible Reactions of Gaseous Ions. 7. Hydrogen Systems. *J. Am. Chem. Soc.* **1972**, *94*, 8669–8672.
- (10) Elford, M. T.; Milloy, H. B. Mobility of H_3^+ and H_5^+ Ions in Hydrogen and Equilibrium Constant for Reaction $H_3^+ + 2H_2$ Reversible $H_5^+ + H_2$ at Gas Temperatures of 195, 273 and 293K. *Aust. J. Phys.* **1974**, *27*, 795–811.
- (11) Less, A. B.; Rol, P. K. Merging Beams Study of the $H_3^+(D_2, H_2)HD_2^+$ Reaction Mechanism. *J. Chem. Phys.* **1975**, *63*, 5077–5081.
- (12) Johnsen, R.; Huang, C. M.; Biondi, M. A. 3-Body Association Reactions of H^+ and H_3^+ Ions in Hydrogen from 135 to 300K. *J. Chem. Phys.* **1976**, *65*, 1539–1542.
- (13) Elford, M. T. The Heat of Dissociation of H_5^+ Derived from Measurements of Ion Mobilities. *J. Chem. Phys.* **1983**, *79*, 5951–5960.
- (14) Beuhler, R. J.; Ehrenson, S.; Friedman, L. Hydrogen Cluster Ion Equilibria. *J. Chem. Phys.* **1983**, *79*, 5982–5991.
- (15) Giles, K.; Adams, N. G.; Smith, D. A Study of the Reactions of H_3^+ , H_2D^+ , HD_2^+ , and D_3^+ with H_2 , HD , and D_2 Using a Variable Temperature Selected Ion Flow Tube. *J. Phys. Chem.* **1992**, *96*, 7645–7650.
- (16) Cordonnier, M.; Uy, D.; Dickson, R. M.; Kerr, K. E.; Zhang, Y.; Oka, T. Selection Rules for Nuclear Spin Modifications in Ion-Neutral Reactions Involving H_3^+ . *J. Chem. Phys.* **2000**, *113*, 3181–3193.
- (17) Gerlich, D.; Herbst, E.; Roueff, E. $H_3^+ + HD \leftrightarrow H_2D^+ + H_2$: Low-Temperature Laboratory Measurements and Interstellar Implications. *Planet Space Sci.* **2002**, *50*, 1275–1285.
- (18) Hugo, E.; Asvany, O.; Schlemmer, S. $H_3^+ + H_2$ Isotopic System at Low Temperatures: Microcanonical Model and Experimental Study. *J. Chem. Phys.* **2009**, *130*, 164302/1–21.
- (19) Hiraoka, K. A Determination of the Stabilities of $H_3^+(H_2)_n$ with $n=1-9$ from Measurements of the Gas-Phase Ion Equilibria $H_3^+(H_2)_{n-1} + H_2 = H_3^+ + (H_2)_n$. *J. Chem. Phys.* **1987**, *87*, 4048–4055.
- (20) Kirchner, N. J.; Bowers, M. T. Fragmentation Dynamics of Metastable Hydrogen-Ion Cluster H_5^+ , H_7^+ , and H_9^+ — Experiment and Theory. *J. Phys. Chem.* **1987**, *91*, 2573–2582.
- (21) Paul, W.; Schlemmer, S.; Lücke, B.; Gerlich, D. Deuteration of Positive Hydrogen Cluster Ions H_5^+ to H_17^+ at 10K. *Chem. Phys.* **1996**, *209*, 265–274.
- (22) Oka, T. Observation of the Infrared Spectrum of H_3^+ . *Phys. Rev. Lett.* **1980**, *45*, 531–534.
- (23) Oka, T. The Infrared Spectrum of H_3^+ in Laboratory and Space Plasmas. *Rev. Mod. Phys.* **1992**, *64*, 1141–1149.
- (24) Geballe, T. R.; Oka, T. Detection of H_3^+ in Interstellar Space. *Nature* **1996**, *384*, 334–335.
- (25) Lindsay, C. M.; McCall, B. J. Comprehensive Evaluation and Compilation of H_3^+ Spectroscopy. *J. Mol. Spectrosc.* **2001**, *210*, 60–83.
- (26) Geballe, T. R.; Oka, T. A Key Molecular Ion in the Universe and in the Laboratory. *Science* **2006**, *312*, 1610–1612.
- (27) Oka, T. Interstellar H_3^+ . *Proc. Natl. Acad. Sci. U.S.A.* **2006**, *103*, 12235–12242.
- (28) Yamaguchi, Y.; Gaw, J. F.; Remington, R. B.; Schaefer, H. F., III. The H_5^+ Potential Energy Hypersurface — Characterization of 10 Distinct Energetically Low-Lying Stationary-Points. *J. Chem. Phys.* **1987**, *86*, 5072–5081.
- (29) Kraemer, W. P.; Spirko, V.; Bludsky, O. Extended Ab Initio Study of the Vibrational Dynamics of H_5^+ and D_5^+ Including All Vibrational Modes. *J. Mol. Spectrosc.* **1994**, *165*, 500–509.
- (30) Stich, I.; Marx, D.; Parrinello, M.; Terakura, K. Protonated Hydrogen Clusters. *J. Chem. Phys.* **1997**, *107*, 9482–9492.
- (31) Chermette, H.; Ymmud, I. V. Structure and Stability of Hydrogen Clusters up to H_{21}^+ . *Phys. Rev. B* **2001**, *63*, 165427/1–10.
- (32) Barbatti, M.; Jalbert, G.; Nascimento, M. A. C. The Structure and Thermochemical Properties of the $H_3^+(H_2)_n$ Clusters ($n=8-11$). *J. Chem. Phys.* **2001**, *114*, 7066–7072.
- (33) Barbatti, M.; Nascimento, M. A. C. Vibrational Analysis of Small H_n^+ Hydrogen Clusters. *J. Chem. Phys.* **2003**, *119*, 5444–5448.
- (34) Prosmi, R.; Villarreal, P.; Delgado-Barrio, G. Structures and Energetic of H_n^+ Clusters ($n = 5-11$). *J. Phys. Chem. A* **2003**, *107*, 4768–4772.
- (35) Ohta, Y.; Ohta, K.; Kinugawa, K. Quantum Effect on the Internal Proton Transfer and Structural Fluctuation in the H_5^+ Cluster. *J. Chem. Phys.* **2004**, *121*, 10991–10999.
- (36) Xie, Z.; Braams, B. J.; Bowman, J. M. Ab Initio Global Potential-Energy Surfaces for $H_5^+ \rightarrow H_3^+ + H_2$. *J. Chem. Phys.* **2005**, *122*, 224307/1–7.
- (37) Spirko, V.; Amano, T.; Kraemer, W. P. Vibrational Predissociation of H_5^+ . *J. Chem. Phys.* **2006**, *124*, 244303/1–5.
- (38) e Silva, G. M.; Gargano, R.; da Silva, W. B.; Roncaratti, L. F.; Acioli, P. H. Quantum Monte Carlo and Genetic Algorithm Study of the Potential Energy Surface of the H_5^+ Molecule. *Int. J. Quantum Chem.* **2007**, *108*, 2318–2325.
- (39) Acioli, P. H.; Xie, Z.; Braams, B. J.; Bowman, J. M. Vibrational Ground State Properties of H_5^+ and Its Isotopomers from Diffusion Monte Carlo Calculations. *J. Chem. Phys.* **2008**, *128*, 104318/1–6.
- (40) Aguado, A.; Barragán, P.; Prosmi, R.; Delgado-Barrio, G.; Villarreal, P.; Roncero, O. A New Accurate and Full Dimensional Potential Energy Surface for H_5^+ Based on a Triatomics-in-Molecules Analytic Functional Form. *J. Chem. Phys.* **2010**, *133*, 024306/1–15.
- (41) (a) Barragán, P.; Prosmi, R.; Roncero, O.; Aguado, A.; Villarreal, P.; Delgado-Barrio, G. Towards a Realistic Density Functional Theory Potential Energy Surface for the H_5^+ Cluster. *J. Chem. Phys.* **2010**, *133*, 054303/1–10. (b) Sanz-Sanz, C.; Roncero, O.; Valdés, A.; Prosmi, R.; Delgado-Barrio, G.; Villarreal, P.; Barragán, P.; Aguado, A. Infrared Spectrum of H_5^+ and D_5^+ : The Simplest Shared-Proton Model. *Phys. Rev. A* **2011**, *84*, 060502/1–4. (c) Aguado, A.; Sanz-Sanz, C.; Villarreal, P.; Roncero, O. Simulation of the Infrared Predissociation Spectra of H_5^+ . *Phys. Rev. A* **2012**, *85*, 032514/1–16.
- (42) De Tudela, R. P.; Barragán, P.; Prosmi, R.; Villarreal, P.; Delgado-Barrio, G. Internal Proton Transfer and H_2 Rotations in the H_5^+ Cluster: A Marked Influence on Its Thermal Equilibrium State. *J. Phys. Chem. A* **2011**, *115*, 2483–2488.
- (43) McGuire, B. A.; Wang, Y.; Bowman, J. M.; Widicus-Weaver, S. I. Do H_5^+ and Its Isotopologues Have Rotational Spectra? *J. Phys. Chem. Lett.* **2011**, *2*, 1045–1047.
- (44) Valdez, A.; Prosmi, R.; Delgado-Barrio, G. Quantum-Dynamics Study of the H_5^+ Cluster: Full Dimensional Benchmark Results on Its Vibrational States. *J. Chem. Phys.* **2012**, *136*, 104302/1–6.
- (45) Okumura, M.; Yeh, L. I.; Lee, Y. T. The Vibrational Predissociation Spectroscopy of Hydrogen Cluster Ions. *J. Chem. Phys.* **1985**, *83*, 3075–3076.
- (46) Okumura, M.; Yeh, L. I.; Lee, Y. T. Infrared-Spectroscopy of the Cluster Ions $H_3^+(H_2)_n$. *J. Chem. Phys.* **1988**, *88*, 79–91.

(47) Cheng, T. C.; Bandyopadhyay, B.; Wang, Y.; Carter, S.; Braams, B. J.; Bowman, J. M.; Duncan, M. A. Shared-Proton Mode Lights up the Infrared Spectrum of Fluxional Cations H_5^+ and D_5 . *J. Phys. Chem. Lett.* **2010**, *1*, 758–762.

(48) Oepts, D.; van der Meer, A. F. G.; van Amersfoort, P. W. The Free-Electron-Laser User Facility FELIX. *Infrared Phys. Technol.* **1995**, *36*, 297–308.

(49) (a) Okumura, M.; Yeh, L. I.; Myers, J. D.; Lee, Y. T. Infrared Spectra of the Cluster Ions $\text{H}_7\text{O}_3^+\cdot\text{H}_2$, $\text{H}_9\text{O}_4^+\cdot\text{H}_2$. *J. Chem. Phys.* **1986**, *85*, 2328–2329. (b) Okumura, M.; Yeh, L. I.; Myers, J. D.; Lee, Y. T. Infrared Spectra of the Solvated Hydronium Ion: Vibrational Predissociation Spectroscopy of Mass-Selected $\text{H}_3\text{O}^+(\text{H}_2\text{O})_n(\text{H}_2)_m$. *J. Phys. Chem.* **1990**, *94*, 3416–3427.

(50) Ebata, T.; Fujii, A.; Mikami, N. Vibrational Spectroscopy of Small-Sized Hydrogen-Bonded Clusters and Their Ions. *Int. Rev. Phys. Chem.* **1998**, *17*, 331–361.

(51) Bieske, E. J.; Dopfer, O. High-Resolution Spectroscopy of Cluster Ions. *Chem. Rev.* **2000**, *100*, 3963–3998.

(52) Robertson, W. H.; Johnson, M. A. Molecular Aspects of Halide Hydration: The Cluster Approach. *Annu. Rev. Phys. Chem.* **2003**, *54*, 173–213.

(53) Duncan, M. A. Infrared Spectroscopy to Probe Structure and Dynamics in Metal Ion–Molecule Complexes. *Int. Rev. Phys. Chem.* **2003**, *22*, 407–435.

(54) Bagratashvili, V. N.; Letokhov, V. S.; Makarov, A. A.; Ryabov, E. A. *Multiple Photon Infrared Laser Photophysics and Photochemistry*; Harwood Academic Publishers: Chur, Switzerland, 1985.

(55) Oomens, J.; Sartakov, B. G.; Meijer, G.; von Helden, G. Gas-Phase Infrared Multiple Photon Dissociation Spectroscopy of Mass-Selected Molecular Ions. *Int. J. Mass Spectrom.* **2006**, *254*, 1–19.

(56) Asmis, K. R.; Fielicke, A.; von Helden, G.; Meijer, G. Atomic Clusters: From Gas Phase to Deposited. *Chem. Phys. Solid Surf.* **2007**, *12*, 327–375.

(57) Asmis, K.; Neumark, D. M.; Bowman, J. M. Gas Phase Vibrational Spectroscopy of Strong Hydrogen Bonds. In *Hydrogen Transfer Reactions: Physical and Chemical Aspects*; Hynes, J. T., Klinman, J. P., Limbach, H.-H., Schowen, R. L., Eds.; Wiley-VCH: Weinheim, Germany, 2007; Vol. 1, pp 53–76.

(58) Hamilton, S. M.; Hopkins, W. S.; Harding, D. J.; Walsh, T. R.; Haertelt, M.; Kerpel, C.; Gruene, P.; Meijer, G.; Fielicke, A.; Mackenzie, S. R. Infrared-Induced Reactivity of N_2O on Small Gas-Phase Rhodium Clusters. *J. Phys. Chem. A* **2011**, *115*, 2489–2497.

(59) Asmis, K. R.; Pivonka, N. L.; Santambrogio, G.; Brummer, M.; Kaposta, C.; Neumark, D. M.; Wöste, L. Gas-Phase Infrared Spectrum of the Protonated Water Dimer. *Science* **2003**, *299*, 1375–1377.

(60) Headrick, J. M.; Diken, E. G.; Walters, R. S.; Hammer, N. I.; Christie, R. A.; Cui, J.; Myshakin, E. M.; Duncan, M. A.; Johnson, M. A.; Jordan, K. D. Spectral Signatures of the Hydrated Proton Vibrations in Water Clusters. *Science* **2005**, *308*, 1765–1769.

(61) Vendrell, O.; Gatti, F.; Meyer, H.-D. Dynamics and Infrared Spectroscopy of the Protonated Water Dimer. *Angew. Chem., Int. Ed.* **2007**, *46*, 6918–6921.

(62) Irimia, D.; Dobrikov, D.; Kortekaas, R.; Voet, H.; van den Ende, D. A.; Groen, W. A.; Janssen, M. H. M. A Short Pulse (7 μs FWHM) and High Repetition Rate (dc-5kHz) Cantilever Piezovalve for Pulsed Atomic and Molecular Beams. *Rev. Sci. Instrum.* **2009**, *80*, 113303/1–6.

(63) Goebbert, D. J.; Meijer, G.; Asmis, K. R. 10 K Ring Electrode Trap-Tandem Mass Spectrometer for Infrared Spectroscopy of Mass Selected Ions. *AIP Conf. Proc.* **2009**, *1104*, 22–29.

(64) Goebbert, D. J.; Wende, T.; Bergmann, R.; Meijer, G.; Asmis, K. R. Messenger-Tagging Electrosprayed Ions: Vibrational Spectroscopy of Suberate Dianions. *J. Phys. Chem. A* **2009**, *113*, 5874–5880.